

# An Age-Structured Model for Erythropoiesis following a Phlebotomy

Joseph M. Mahaffy<sup>\*†</sup>      Samuel W. Polk<sup>\*‡</sup>  
Roland K. W. Roeder<sup>\*§</sup>

**CRM-2598**

February 1999

---

<sup>\*</sup>Department of Mathematical Sciences, San Diego State University, San Diego, CA 92182-0314, U.S.A.

<sup>†</sup>The work of this author was supported in part by NSF grant DMS-9208290 and Centre de recherches mathématiques, Université de Montréal, Montréal, Québec H3C 3J7.

<sup>‡</sup>The work of this author was supported under the MARC/RCMS program of NIH by grant 5-34-GM08303-04.

<sup>§</sup>The work of this author was supported under the REU program of NSF by grant DMS-9208290.



## Abstract

This study examines an age-structured model for erythropoiesis following a phlebotomy on normal human subjects. The model extends previous work to include the variable velocity of maturation and the effects of plasma on hematocrit. Experimental data on phlebotomized subjects are used to fit the parameters in the model, and various numerical simulations are performed. The numerical studies are compared to previous models for humans following a blood donation and rabbits with an induced autoimmune hemolytic anemia. The variable aging of precursors to erythrocytes results in increased stability of the model, especially for the anemic rabbit simulations. The relative importance of the various controls in the model and their physiological significance are discussed. Experimental hematocrit readings on two of the authors suggest more complicated controls.

*Key words:* age-structured model, erythropoiesis, phlebotomy, autoimmune hemolytic anemia, state-dependent delay differential equations, method of characteristics, numerical simulations

## Résumé

Un modèle d'érythropoïèse avec structure d'âge est utilisé pour déterminer les conséquences d'une phlébotomie chez des sujets humains. Ce modèle généralise un travail précédent, par l'ajout d'une vitesse de maturation variable et les considérations distinctes du plasma et des hématocrites. Des données expérimentales recueillies chez des donneurs sont employées pour ajuster les paramètres du modèle et effectuer des simulations numériques : ces dernières sont comparées au modèle précédent, chez l'humain suite à un don de sang, et chez le lapin atteint d'anémie hémolytique auto-immune induite. La plasticité du vieillissement des cellules précurseuses aux érythrocytes augmente la stabilité des solutions stationnaires dans le modèle, surtout chez le lapin. L'importance relative des divers mécanismes de contrôle dans le modèle, de même que leur signification physiologique, sont discutées. Une comparaison avec des données recueillies chez deux des auteurs indique une plus grande complexité des mécanismes de contrôle dans le système réel.



# 1 Introduction

The advent of the serious disease AIDS has caused great concern about the HIV virus infecting the blood supplies around the world. Each day 40,000 units (450 g) of blood are needed in the U.S. [1], yet no artificial substitute has been created. This means that blood donations remain a critical life-giving source for the many operations and replacements needed after massive hemorrhages from accidents or treatment of diseases like hemophilia. A better understanding of the regulation of erythropoiesis through modeling may provide valuable information on optimal collection schemes for autologous donors who want to guarantee a safe blood supply or help increase supplies in the case of a major disaster.

There are several hematopoietic diseases that are believed to arise due to abnormalities in the feedback controls regulating hematopoiesis [7, 16, 17, 18, 20, 21, 22, 23, 28, 34, 39, 41, 42, 43]. For example, oscillations in the erythrocyte concentrations are observed in cases of autoimmune hemolytic anemia [12, 30, 32]. An age-structured model of Bélair *et al.* [2] and Mahaffy *et al.* [25] reasonably reproduced the experimental results of Orr *et al.* [30] for rabbits that were given red blood cell iso-antibodies over a long period of time, inducing an autoimmune hemolytic anemia. The mathematical models provide an alternate tool for understanding the relative importance of the different physiological controls and could be used to test therapeutic treatments.

Erythropoiesis is the genesis of undifferentiated stem cells, primarily in the bone marrow, to mature red blood cells, or erythrocytes, which circulate throughout the body to deliver oxygen ( $O_2$ ) to the tissues. (*William's Hematology* [3] provides an excellent reference for erythropoiesis.) The primary control of erythropoiesis is governed by the hormone erythropoietin (Epo), which is released in the bloodstream based on a negative feedback mechanism that detects the partial pressure of  $O_2$  in the blood. The concentration of Epo directly affects precursor cells (BFU-Es and CFU-Es) by determining the number that mature into erythrocytes through either recruitment or preventing apoptosis. In addition, Epo appears to accelerate the maturing process when the hematocrit is particularly low.

The regulation of erythropoiesis has been studied extensively using age-structured models [2, 4, 5, 6, 13, 14, 25, 26]. Bélair *et al.* [2] and Mahaffy *et al.* [25] used several assumptions to reduce their age-structured models to models with delays that allowed bifurcation analysis and relatively simple numerical studies. This work extends the mathematical model developed in Mahaffy *et al.* [25] to include the effects of plasma on the regulation of erythropoiesis following a phlebotomy. After a phlebotomy, the body loses both erythrocytes and plasma. However, the  $O_2$  detection, which determines the quantity of Epo released, probably depends on the concentration of hemoglobin in the blood. The model of Mahaffy *et al.* [25] is modified to examine the concentration of hemoglobin, then numerical studies find parameter values that best fit the experimental studies of Maeda *et al.* [24] and Wadsworth [38] for a collection of normal males following a phlebotomy.

The complete age-structured model includes a variable velocity of aging for the precursor cells, which has been observed experimentally ([3], p.436). This effect significantly increases the difficulty of study, as the model no longer reduces to a relatively simple system of delay differential equations. To analyze a variable velocity of aging, the system of partial differential equations is simulated numerically. Our numerical studies use a modification of the method of characteristics presented by Sulsky [36, 37] for age-structured models and compare the results to the simplified model discussed above. Our analysis of the mathematical model simulating the experiment of Orr *et al.* [30] for an induced autoimmune hemolytic anemia in rabbits shows that creating the initial data for the system of delay differential equations is fairly complex compared to the initial conditions for the partial differential equations. However, the partial differential equation code is significantly more complex and requires smaller stepsizes for a given accuracy. Including the variable velocity of aging for precursor cells stabilizes the mathematical model, suggesting the importance of this adaptation to physiological controls.

In the next section we briefly present crucial elements of the physiology used to formulate the age-structured model, including the changes from the previous age-structured models of Bélair *et al.* [2] and Mahaffy *et al.* [25]. Several assumptions are necessary to reduce the age-structured model to a system of state-dependent delay differential equations. The third section begins with a least squares best fit of the

simplified delay differential equation model to the collective experimental data of normal males following a phlebotomy. A numerical scheme based on the method of characteristics is developed to study the complete age-structured model, including the complication caused by a variable velocity of aging. When the velocity of aging of the precursor cells is allowed to vary, the numerical simulations show increased stability of the model. The periodic oscillations in a simulation for a rabbit with an induced autoimmune hemolytic anemia are eliminated by this change to the model. The final section contains actual data collected on two of the authors following a phlebotomy, and these data show additional complications in the physiological controls for the concentration of erythrocytes in the blood. We discuss the relevance of our mathematical model to normal subjects following a phlebotomy and to diseased states, such as a hemolytic anemia.

## 2 Mathematical Model for a Phlebotomy

This section summarizes key elements in the physiology of erythropoiesis and develops a mathematical model describing this process, especially following a significant blood loss. The model and its associated assumptions closely parallel the earlier works of Bélair *et al.* [2] and Mahaffy *et al.* [25]. After a phlebotomy, the body has lost about 450 g of whole blood, which is about 8% of total blood volume for the average man. About 43% of the blood by volume ([3], p.426) is erythrocytes with most of the remainder being plasma. The plasma is replaced fairly rapidly; however, the erythrocytes require the much longer process of erythropoiesis to regenerate. Since biological controls usually react to concentration changes, the model developed here differs from the earlier models by examining the hematocrit or hemoglobin concentration instead of the direct population of erythrocytes. This requires the addition of a function for the plasma component in whole blood.

Since this model extends earlier models [2, 25], we significantly condense the physiological information used to develop the age-structured model. Erythropoiesis begins with either the pluripotential stem cell or a self-sustaining pool of BFU-Es (burst forming units already committed to become erythrocytes). Primarily from the influence of the hormone erythropoietin, Epo, precursor cells mature in about 6 days to become mature erythrocytes. Erythrocytes are specialized cells containing hemoglobin that transport  $O_2$  from the lungs to the other tissues in the body. Specific cells, primarily the peritubular interstitial cells of the outer cortex in the kidneys, sense the partial pressure of  $O_2$  in the blood and release Epo using negative feedback to complete this physiological control loop.

Since the process of erythropoiesis depends on the relatively long maturation and finite life-span of the erythrocytes, an age-structured model provides a natural means of studying this population of cells. The age-structured model begins with the population of precursor cells, denoted  $p(t, \mu)$ , where  $t$  is the simulation time and  $\mu$  is the age of the precursor cells and could represent accumulation of hemoglobin. Experiments suggest that Epo affects the early stages of erythropoiesis in two significant ways. Its primary control is on the number of new cells recruited into the proliferating precursor population, probably by preventing apoptosis of CFU-Es. Let  $S_0(E)$  represent the number of new precursor cells, which are recruited and survive into the proliferating precursor cell population. Epo also appears to accelerate the maturing process, so let  $V(E)$  be the velocity of maturation. This information combines to give the boundary condition:

$$V(E)p(t, 0) = S_0(E). \quad (2.1)$$

In general, the birth rate for the proliferating precursor cells depends on the level of maturity,  $\mu$ , and the concentration of Epo and is denoted  $\beta(\mu, E)$ . If  $\kappa(\mu - \bar{\mu})$  is the distribution of maturity levels of the cells that are released into the circulating blood, where  $\bar{\mu}$  represents the mean age of mature precursor cells and  $\mu_F$  is the maximum age of a precursor cell, then

$$\int_0^{\mu_F} \kappa(\mu - \bar{\mu}) d\mu = 1,$$

and the disappearance rate function is given by:

$$\mathcal{K}(\mu) = \frac{\kappa(\mu - \bar{\mu})}{\int_{\mu}^{\mu_F} \kappa(s - \bar{\mu}) ds}.$$

Experiments of Finch *et al.* [9] show that following a significant blood loss, there is an early release of stored reticulocytes, called “shift reticulocytes.” Thus, a better model might have  $\mathcal{K}$  depend on either Epo or the concentration of mature cells. Our  $V(E)$  partially accounts for this phenomenon. With these conditions the age-structured model for the population of precursor cells with  $t > 0$  and  $0 < \mu < \mu_F$  satisfies:

$$\frac{\partial p}{\partial t} + V(E) \frac{\partial p}{\partial \mu} = V(E)[\beta(\mu, E)p - \mathcal{K}(\mu)p]. \quad (2.2)$$

The last stage of development for precursor cell is the non-proliferative phase, where the cells now called reticulocytes become packed with hemoglobin and lose many other cellular components, including their nuclei. These cells actually shrink in size to where they squeeze out of the bone marrow and enter the blood stream as mature erythrocytes, which serve as transporters of  $O_2$  to the tissues of the body. Let  $m(t, \nu)$  be the population of erythrocytes in the blood at time  $t$  and age  $\nu$ . If the mature cells age at a rate  $W$ , which is almost constant for erythropoiesis since the aging process appears to depend only on the number of times that an erythrocyte passes through the capillaries, then the boundary condition for cells entering the mature population is given by the following expression:

$$Wm(t, 0) = V(E) \int_0^{\mu_F} \kappa(\mu - \bar{\mu})p(t, \mu) d\mu. \quad (2.3)$$

After many times of being squeezed through the capillaries, the oldest erythrocytes lose pliability of their membranes, which cannot be repaired without a nucleus. Since these cells could cause damage to the circulatory system by blocking blood vessels, the oldest erythrocytes are marked for active degradation by macrophages. Assuming either a constant supply of markers or number of phagocytes that are satiated from engulfing the oldest erythrocytes results in a constant flux of erythrocytes from the mature population. This produces a moving boundary condition with the age of the oldest erythrocyte,  $\nu_F(t)$ , varying in  $t$ . The boundary condition, following Mahaffy *et al.* [25], is given by:

$$(W - \dot{\nu}_F(t))m(t, \nu_F(t)) = Q, \quad (2.4)$$

where  $Q$  is the fixed erythrocyte removal rate. A number of erythrocytes from all age classes are lost primarily from the breakage of capillaries due to body movement or physical impact such as that caused by feet hitting a hard surface while running. Let  $\gamma(\nu)$  be the death rate of mature cells (depending only on age), then the age-structured model describing  $m(t, \nu)$  is given by:

$$\frac{\partial m}{\partial t} + W \frac{\partial m}{\partial \nu} = -W\gamma(\nu)m, \quad t > 0, \quad 0 < \nu < \nu_F(t), \quad (2.5)$$

where the maximum age,  $\nu_F(t)$ , is determined by (2.4).

The ability of blood to carry  $O_2$  to the tissues is more complicated than the simple counting of erythrocytes in the blood. A standard phlebotomy for a normal male entails about an 8% loss in total blood volume with 43% of that volume on average being erythrocytes. (Females have a lower average hematocrit with greater variability due to their body tissue composition and menstrual cycle and lose a higher percentage of blood volume from their smaller size. [27]) The initial response of the body is to shunt blood away from less important tissues, which means vital organs such as the kidneys where the majority of the  $O_2$  sensors reside will see no significant drop in the partial pressure of  $O_2$ . There are  $O_2$  sensors in the skin from which the blood is shunted, but our model does not consider this. A better measure of the  $O_2$  carrying ability of the blood and the test used by blood banks is the concentration of hemoglobin, which is the actual  $O_2$  carrying molecule. Another related quantity is the hematocrit, which is the percent of the

blood volume comprised of erythrocytes. Since the concentration of hemoglobin in erythrocytes is almost constant, there is a strong correlation between these measurements. Thus, the blood's O<sub>2</sub> carrying capacity is directly related to the hematocrit,  $H(t)$ , or hemoglobin,  $Hb(t)$ , which are given by:

$$H(t) = \frac{M(t)}{M(t) + q(t)} \quad \text{and} \quad Hb(t) \simeq \frac{100}{3}H(t), \quad (2.6)$$

where  $M(t)$  is the total volume of erythrocytes and  $q(t)$  is the plasma volume. With the assumption that all erythrocytes are similar in volume, independent of age, the erythrocyte volume correlates directly to the total population of mature cells, so

$$M(t) = \int_0^{\nu_F(t)} m(t, \nu) d\nu, \quad (2.7)$$

and  $M$  has volume units equivalent to the average size of the erythrocyte.

The plasma volume is more rapidly generated. First, interstitial fluid enters blood vessels to increase blood volume, then with hydration the blood generates new serum proteins with significant increases in liver albumin synthesis after 36 hr, creating new plasma. Moore [27] states that following a large blood loss, plasma begins entering the blood on average at 40-60 ml/hr and stabilizes exponentially in 30-40 hr. This blood volume change occurs primarily at the expense of the interstitial volume, which takes several days to recover. The data of Wadsworth [38] suggests that the new plasma increases blood volume to a level higher than before the phlebotomy. From these data, we chose the plasma function

$$q(t) = \alpha_1(1 + (\alpha_2 t - 0.08)e^{-\alpha_3 t}), \quad (2.8)$$

where 0.08 reflects the plasma lost at  $t = 0$  (time of the phlebotomy) and  $\alpha_1$  normalizes the plasma volume with the erythrocyte volume  $M$ . The parameters  $\alpha_2$  and  $\alpha_3$  are found in the next section using a least squares best fit to the data of Maeda *et al.* [24] and Wadsworth [38].

The Epo level  $E$  is governed by a differential equation with a negative feedback, depending on the hematocrit,  $H(t)$ , or hemoglobin,  $Hb(t)$ , which reflects O<sub>2</sub> carrying capacity of the blood. Since most data give the concentration of hemoglobin, the equation used in our model is given by

$$\frac{dE}{dt} = f(Hb) - kE, \quad (2.9)$$

where  $k$  is the decay constant for the hormone and  $f(Hb)$  is a monotone decreasing function of  $Hb$ , representing the negative feedback effect of the O<sub>2</sub> carrying capacity of the blood on the rate of hormone production. We choose the Hill function  $f$ :

$$f(Hb) = \frac{a}{1 + K(Hb)^r}, \quad (2.10)$$

which often occurs in enzyme kinetic problems. Bélair *et al.* [2] used experimental data in the literature to find the parameter  $r$ , while the parameters  $a$  and  $K$  are found in the beginning of the next section by a least-squares estimate.

Mahaffy *et al.* [25] analyzed the partial differential equations and their boundary conditions given by Eqns. (2.1)–(2.5), which describe an age-structured model for the erythrocytes. The method of characteristics is applied to this system following the techniques of several authors [2, 10, 11, 25, 26, 35] to produce a system of threshold delay equations. The method of characteristics is also the basis of the numerical scheme for solving the partial differential equations in the next section.

In their general form, Eqns. (2.1)–(2.9) are too complicated to analyze and fit to experimental data. Mahaffy *et al.* [25] made several simplifying assumptions that are reasonable for erythropoiesis, which allowed reduction of the system of threshold delay equations to a system of delay differential equations with a fixed delay in one equation and a state dependent delay in an equation governing the age at

which mature erythrocytes die. Our analysis of the age-structured model for erythropoiesis following a phlebotomy begins with very similar assumptions to fit the experimental data and connect to the previous research [2, 25], then it relaxes the condition on the velocity of aging to better match known effects of Epo and determine how much this affects the model through computer simulation.

Following Mahaffy *et al.* [25], we assume that the velocities of aging are constant and normalized to one, *i.e.*,

$$V(E) = 1 \quad \text{and} \quad W = 1.$$

This assumption significantly simplifies the expressions for  $p(t, \mu)$  and  $m(t, \nu)$ . The second assumption is that the precursor cells grow exponentially for a given period of time  $\mu_R$ , then stop dividing as seen in the physiological system. This assumption on the birth rate of the precursor cells yields

$$\beta(\mu, E) = \begin{cases} \beta, & \mu < \mu_R, \\ 0, & \mu \geq \mu_R, \end{cases} \quad (2.11)$$

for some constant growth rate  $\beta$ . If  $\kappa(\mu - \bar{\mu})$  is a Dirac  $\delta$ -function, then the changing of precursor cells into mature erythrocytes only occurs on the boundary. Finally, the death rate of the mature cells,  $\gamma(\nu)$ , is taken to be constant. From Mahaffy *et al.* [25], these assumptions reduce the age-structured model to the following system of delay differential equations with a fixed delay  $T$  and a state dependent delay occurring in the equation governing the age at which mature cells die:

$$\begin{aligned} \frac{dM(t)}{dt} &= e^{\beta\mu_R} S_0(E(t-T)) - \gamma M(t) - Q, \\ \frac{dE(t)}{dt} &= f(Hb(t)) - kE(t), \\ \frac{d\nu_F(t)}{dt} &= 1 - \frac{Qe^{-\beta\mu_R} e^{\gamma\nu_F(t)}}{S_0(E(t-T-\nu_F(t)))}. \end{aligned} \quad (2.12)$$

Note that  $Hb(t)$  in the second differential equation is found by Eqns. (2.6) and (2.8).

As noted in Mahaffy *et al.* [25], the system of equations (2.12) is relatively easy to analyze. The first two differential equations are uncoupled from the state-dependent delay in the  $\dot{\nu}_F(t)$  equation. Thus, bifurcation analysis is reduced to examining a system of two differential equations with a single time delay,  $T$ . Furthermore, this system of delay differential equations is readily simulated using an adaptation of the fourth order Runge-Kutta for ordinary differential equations. This latter fact significantly simplifies our problem of fitting parameters in the model to the experimental data.

### 3 Numerical Simulation of the Model

The model derived in the previous section was developed to examine the controls of the erythropoietic system following a phlebotomy. Blood banks require eight weeks between blood donations, but could a more optimal strategy be developed for crisis periods requiring increased blood supplies or could autologous donors wanting the safety of their own blood during optional surgery obtain a larger supply? Several experiments have collected data on hemoglobin and Epo concentrations for human subjects following a phlebotomy. To test the age-structured model developed in the previous section, we need data over several weeks, so the data of Maeda *et al.* [24] and Wadsworth [38] were combined. These data and some physiological information were sufficient to identify the many parameters in the simplified model (2.12) using a least squares best fit. The model fits the collection of data reasonably well, so could be used to examine different blood donation schemes without human subjects. However, the significant variation observed in individual data (as shown in the next section) suggests additional factors be considered.

The studies of (2.12) are extended to test the effects of the state varying velocity  $V(E)$ , which is the key complicating element preventing the reduction of the threshold-type delay differential equations to the simplified system of delay differential equations (2.12). Sulsky [36, 37] showed that one of the most

efficient numerical methods for age-structured models uses the method of characteristics, which is how our age-structured model (2.1)–(2.9) is simplified. When her models included mass-structure [37], which is similar to our model with the state varying velocity, then a combination of the method of characteristics with an adaptive grid scheme was the best numerical routine that she tested.

### 3.1 Parameter Estimation

The analysis of the mathematical model begins with identification of the parameters. The simplified system of delay differential equations (2.12) with the plasma function (2.8) and nonlinear feedback function (2.10) has twelve parameters and the function  $S_0(E)$  to be determined. Bélair *et al.* [2] and Mahaffy *et al.* [25] used information about the human erythropoietic system to find many of the parameters. From cell doubling times and the average time for precursor cells to reach the stage of reticulocytes,  $\beta = 2.079$  (da<sup>-1</sup>) and  $\mu_R = 4.0$  (da). The average loss of erythrocytes, not caused by aging, is assumed to be  $\gamma = 0.001$  (da<sup>-1</sup>). The average time of maturation gives  $T = 6$  (da), while the average mature cell lives 120 (da), which is the equilibrium value for  $\nu_F$ .

Since a normal human subject has  $3.5 \times 10^{11}$  erythrocytes/kg of body weight [8], we assumed the equilibrium value of  $\bar{M} = 3.5$ . From Maeda *et al.* [24], we assumed the initial and equilibrium value of Epo to be 16.95 (mU/ml), while the combined experimental data gave an equilibrium for the concentration of hemoglobin,  $\bar{Hb} = 15.29$  (g/100 ml). With (2.6) and (2.8), the values of  $\bar{M}$  and  $\bar{Hb}$  give  $\alpha_1 = 4.13$ . With the parameter and equilibrium values listed above and the assumption that  $S_0(E)$  is linear, then a steady-state analysis of (2.12) yields  $S_0(E) = 4.45 \times 10^{-7}E$  and  $Q = 0.0275$ . Bélair *et al.* [2] found that the Hill coefficient in (2.10) is  $r = 7$ .

The information above provides all parameters for the simplified model (2.12), except for  $\alpha = (\alpha_2, \alpha_3, a, K)$  and  $k$  in Eqns. (2.8) and (2.10). The parameter  $k$  relates to the half-life of Epo, which literature gives values ranging from 4 to 24 hr, and is computed from the equilibrium conditions on the second equation in (2.12). The four parameters,  $\alpha$ , have no direct biological interpretation, so they were fit to the Maeda *et al.* [24] and Wadsworth [38] data on normal human subjects following a phlebotomy using a least squares functional. The Maeda *et al.* [24] data on Epo concentration have error bars that are ten times the error bars for their hemoglobin concentration. Thus, we chose to give the Epo data only 10% the weighting of the hemoglobin data. Let  $Hb_d(t_i)$  and  $E_d(t_i)$  be the average hemoglobin and Epo concentrations, respectively, of the human subjects at day  $t_i$  and  $Hb(t_i, \alpha)$  and  $E(t_i, \alpha)$  be the solutions of (2.12) depending on the parameters  $\alpha$ . If  $\bar{Hb} = 15.29$  and  $\bar{E} = 16.95$  are used to normalize the data, then the least squares functional to be minimized is given by

$$J(\alpha) = w_m \sum_{i=1}^{N_m} \left( \frac{(Hb_d(t_i) - Hb(t_i, \alpha))^2}{\bar{Hb}} + 0.1 \frac{(E_d(t_i) - E(t_i, \alpha))^2}{\bar{E}} \right) + w_w \sum_{i=1}^{N_w} \left( \frac{(Hb_d(t_i) - Hb(t_i, \alpha))^2}{\bar{Hb}} \right), \quad (3.1)$$

where  $w_m = 8$  and  $w_w = 7$  are the numbers of subjects in the Maeda *et al.* [24] and Wadsworth [38] data, respectively, and  $N_m$  and  $N_w$  are the number of times data were collected. The functional (3.1) was minimized by a computer search over a range of parameter values. For each set of values  $\alpha$ , a modified Runge-Kutta scheme was used to simulate (2.12), then the value of (3.1) was computed and compared to other values of  $\alpha$ . Fig. 3.1 shows the data with the solution  $Hb(t)$  to (2.12) with the optimal parameter values,  $\alpha_2 = 0.05421$ ,  $\alpha_3 = 0.1214$ ,  $a = 198.1$ , and  $K = 9.262 \times 10^{-9}$ . The values of  $\alpha_2$  and  $\alpha_3$  are reasonable based on the information given by Moore [27] and Wadsworth [38]. The equilibrium constraint on  $k$  yields  $k = 4.16$  (da<sup>-1</sup>), which matches the shortest half-life in the literature. The data on the concentration of Epo from Maeda *et al.* [24] are shown with the solution  $E(t)$  to (2.12) in Fig. 3.2.

The Figs. 3.1 and 3.2 show a fairly reasonable fit of the mathematical model to the experimental data. In Fig. 3.1, the data of Maeda *et al.* [24] tend to lie below the curve and show a slower recovery, while the data of Wadsworth [38] are significantly higher in the early part of the experiment (lacking data on the

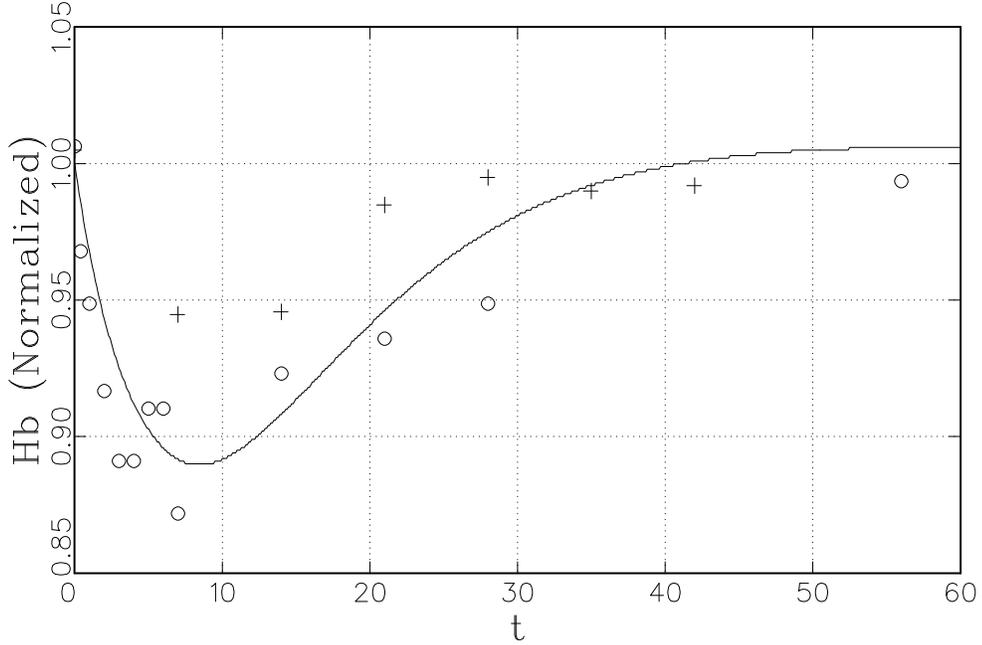


Figure 3.1: Simulation of Eqn. (2.12) with optimal parameters showing the concentration of hemoglobin following a blood donation with data of Maeda *et al.* (○) and Wadsworth (+).

important first few days) and show a more rapid recovery to normal compared to the model. In Fig. 3.2, the Epo data of Maeda *et al.* [24] closely match the model for the first couple weeks, then again his subjects show a slower recovery. We note that these are two distinct experiments with small sample sizes, which complicate the comparisons of our model to the expected response of a normal human subject following a phlebotomy. The mathematical model shows that 90% of the erythrocytes lost from a blood donation are regenerated in slightly more than 30 days. This agrees with the statement in Wadsworth [38] (and often quoted by blood banks) “that recovery of haemoglobin concentration was completed within 3–4 weeks of the haemorrhage.”

### 3.2 Simulation of the Age-Structured Model

With a set of parameters that match the data for the simplified model (2.12), we examined the effects of a variable velocity  $V(E)$  on the system of partial differential equations, (2.1)–(2.9). Our numerical technique parallels Sulsky [37], using the method of characteristics to follow the solution for fixed time steps. When the characteristic velocities  $V(E)$  and  $W$  are one, then the aging of the structured populations move in step with time, which is why the age-structured model readily reduces to the system of delay differential equations. With  $V(E)$  varying with  $E$ , the aging of the precursor population through its accumulation of hemoglobin and advancement to mature erythrocytes changes. Williams ([3], p. 436) claims that under extreme stress, the maturing stage of erythropoiesis is accelerated. Studies using radioiron [9, 15, 19, 31] show that anemic conditions can decrease transit time (time of maturation) in the bone marrow for precursor cells by over a day, and furthermore, the stress of blood loss results in early release of “shift reticulocytes.” In the absence of Epo, the velocity of maturing,  $V(E)$ , should be zero, while at equilibrium it should be one. By assuming that at most maturation is accelerated by two days, we choose a velocity of maturation function of the form:

$$V(E) = \frac{\kappa_1 E}{\kappa_2 + E}, \quad (3.2)$$

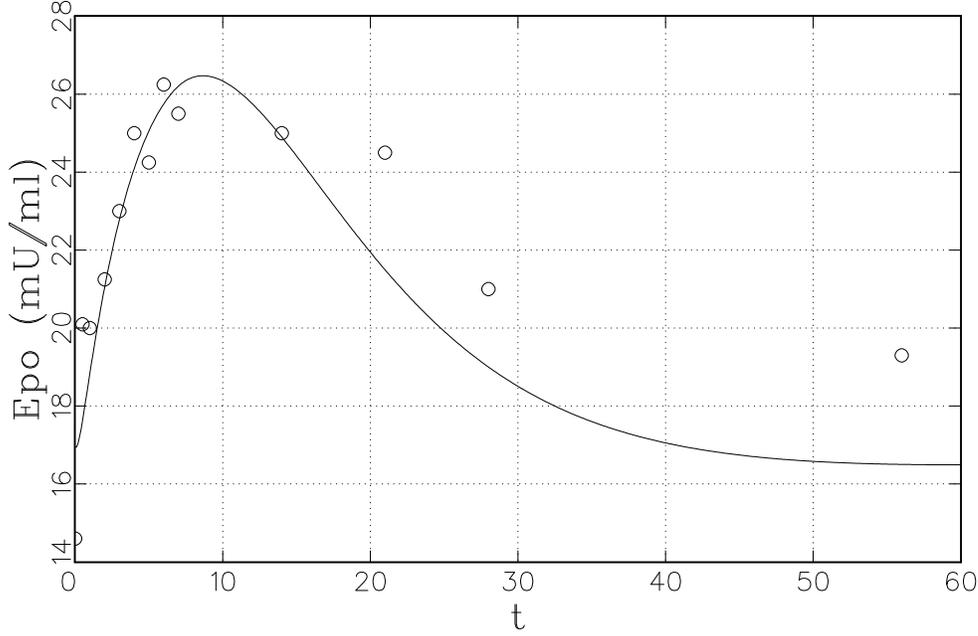


Figure 3.2: Simulation of Eqn. (3.12) showing Epo levels with data of Maeda *et al.* following a blood donation using the optimal parameters found by Eqn. (3.1).

where  $\kappa_1 = 1.5$  and  $\kappa_2 = 8.475$ .

Below we outline the steps used for this numerical computation. The numerical simulation begins with a discretization of the precursor and mature cells denoted

$$p(t_i, \mu_j) \equiv p_{i,j} \quad \text{and} \quad m(t_i, \nu_k) \equiv m_{i,k},$$

where  $t_i = t_0 + ih$  for some step size in time  $h$  and  $\mu_j(i)$  and  $\nu_k$  for appropriate age-structure grids. With the variable velocity, the grid for precursor cells,  $\mu_j(i)$ , varies with time,  $t_i$ . The values  $p_{i,j}$  and  $m_{i,k}$  are referred to as the age classes of cells at time  $t_i$ . In our simulation the normal human subject undergoes a phlebotomy at  $t_0 = 0$ . The initial age classes  $\mu_j(0)$  and  $\nu_k$  are separated by the stepsize  $h$  to give a uniform grid.

The age-structured model is easily solved to find its steady-state cell distribution. At equilibrium,  $V(\bar{E}) = 1$  and with the assumption (2.11), then the precursor cell population has an exponential growth distribution until  $\mu = \mu_R$ , then the cell population remains constant until maturity. Divided into the discrete age classes, the initial precursor population is given by:

$$p_{0,j} = \begin{cases} P_0 e^{\beta \mu_j(0)}, & \mu_j(0) < \mu_R, \\ P_0 e^{\beta \mu_R}, & \mu_j(0) \geq \mu_R, \end{cases},$$

where  $P_0 = S_0(\bar{E})$  is the initial precursor population,  $\mu_R = 4$  (da), and  $\mu_j(0) = jh$  for  $0 \leq j \leq \mu_F/h = J_0$  and  $\mu_F = 6$  for humans.

The steady-state distribution of mature cells is given by  $\bar{m}(\nu) = P_0 e^{\beta \mu_R} e^{-\gamma \nu}$ . At  $t = 0$ , the phlebotomy is assumed to reduce all age classes of mature erythrocytes by 8%. Thus, the initial distribution of mature erythrocytes:

$$m_{0,k} = 0.92 \bar{m}(\nu_k),$$

with  $\nu_k = kh$  for  $0 \leq k \leq \bar{\nu}_F/h$  and  $\bar{\nu}_F = 120$  for humans. After the phlebotomy, the immediate effect on the hemoglobin concentration is no change, since the whole blood donation causes both plasma and erythrocytes to be lost. Hence,  $Hb(0)$  is the same as the equilibrium value.

The method of characteristics is used for subsequent calculations of both the precursor and mature populations. The numerical routine begins by computing  $V(E)$ , using the value of  $E$  from the previous time step. This allows computation of the density of new precursor cells (number of cells/unit age,  $\mu$ ) by

$$p_{i,0} = S_0(E_{i-1})/V(E_{i-1}),$$

where  $i$  represents the index for time. The other precursor population densities are found by following the solutions along the characteristics. Thus, the new grid values,  $\mu_j(i) = \mu_{j-1}(i-1) + hV(E_{i-1})$  for  $1 \leq j \leq J_{i-1} + 1$  and precursor densities at the new grid points are

$$p_{i,j} = \begin{cases} p_{i-1,j-1}e^{\beta hV(E_{i-1})}, & \mu_j(i) < \mu_R, \\ p_{i-1,j-1}, & \mu_j(i) \geq \mu_R, \end{cases},$$

with special consideration for the case where  $\mu_j(i)$  crosses  $\mu_R$  having exponential growth up to  $\mu_R$  and remaining constant afterwards.

The next step in the procedure is finding how many precursor cells enter the mature population. The precursor population densities are integrated over this updated grid using the trapezoid rule to find how many cells are in this new population, including grid values with  $\mu_j(i) > \mu_F$ . The program finds the first  $\mu_j(i) > \mu_F$ . With this value of  $j = J_i$ , the final grid point is adjusted so  $\mu_{J_i} = \mu_F$  and  $p_{i,J_i}$  is given by the weighted average between the values of  $p_{i,J_i-1}$  and  $p_{i,J_i}$  before the grid is adjusted. With this updated grid, the total new precursor population is computed using the trapezoid rule and is subtracted from the total computed before the grid was adjusted. The difference is the number of precursor cells entering the mature population,  $m_{i,0}$ , which satisfies the boundary condition (2.3).

The procedure for finding the populations in the mature age classes,  $m_{i,k}$ , is similar to that for the precursor age classes. However, since  $W = 1$ , the grid  $\nu_k$  remains uniformly spaced with  $\nu_k = hk$  for  $0 \leq k \leq \nu_F(t_i)/h$ , except for the final grid point, which depends on the boundary condition (2.4). The mature age classes at  $t_i$  satisfy

$$m_{i,k} = m_{i-1,k-1}e^{-\gamma h},$$

with each age class decaying exponentially at each time step.

The modeling assumption that a constant number of erythrocytes are destroyed for each time step affects the age of the oldest erythrocytes,  $\nu_F(t)$ , which determines the number of mature age classes. The numerical simulation takes the total number of mature erythrocytes from the previous time step and multiplies it by  $e^{-\gamma h}$  to account for the general loss of erythrocytes from the destruction rate  $\gamma$ , then adds the new cells,  $m_{i,0}$ , entering from the precursor cell population. Next  $hQ$  of the oldest cells are removed with the program finding how many mature age classes remain, including any fractional remainder. Linear interpolation is used to find the new  $\nu_F(t_i)$ .

With the total mature population of erythrocytes,  $M(t_i)$ , known at  $t_i$ , Eqns. (2.6) and (2.8) are used to find the concentration of hemoglobin,  $Hb(t_i)$ . Then Eqn. (2.9) is integrated using an improved Euler's method to find the new concentration of Epo,  $E(t_i)$ . This completes a time step in the simulation and allows computation of all the key variables for any time by iterating the loop.

Due to the complicated nature of this algorithm, traditional error analysis would be difficult. We investigated the maximum difference of  $Hb(t)$  and  $E(t)$ ,  $0 \leq t \leq 60$ , while halving the stepsize. The results indicate Cauchy convergence corresponding to  $O(h)$ , which is to be expected since our code uses an Euler approach to integration. When the stepsize is  $h = 0.02$ , all simulations agree to four significant digits for  $Hb(t)$  and three significant digits for  $E(t)$ , indicating close proximity to the actual solution. The smaller number of significant figures for  $E(t)$  appears to result from  $E(t)$  being sensitive to small errors in  $Hb$  through the feedback function in (2.9) ( $|df(\bar{H}b)/d(Hb)| \simeq 20$ ). For stepsizes below  $h = 0.01$ , computation time became significant, and the increases in roundoff error began to match the decreases in truncation error. For these reasons,  $h = 0.02$  is used for all simulations.

Fig. 3.3 shows a simulation following a blood donation of the complete age-structured model with the variable velocity given in Eqn. (3.2), using a stepsize of  $h = 0.02$ , and compares it to the model given by Eqn. (2.12), where  $V(E) = 1$ . The figure shows that the concentrations of hemoglobin and Epo vary only a few percent over the course of the simulation. If  $Hb(t)$  and  $E(t)$  are solutions with the variable velocity and  $Hb_1(t)$  and  $E_1(t)$  are solutions to (2.12), then the numerical data find that

$$\max_{0 \leq t \leq 50} \frac{|Hb(t) - Hb_1(t)|}{Hb(t)} = 0.0057 \quad \text{and} \quad \max_{0 \leq t \leq 50} \frac{|E(t) - E_1(t)|}{E(t)} = 0.018.$$

The velocity of aging reaches a maximum of  $V(E) = 1.132$  at  $t = 8.3$ . Thus, a relatively large variation in the aging velocity produces relatively minor effects on the concentrations of hemoglobin and Epo. However, the changes do moderate the effect of the blood donation by increasing the minimum concentration of hemoglobin and having the recovery occur slightly earlier as seen by the left shift for the minimum of the graph in Fig. 3.3.

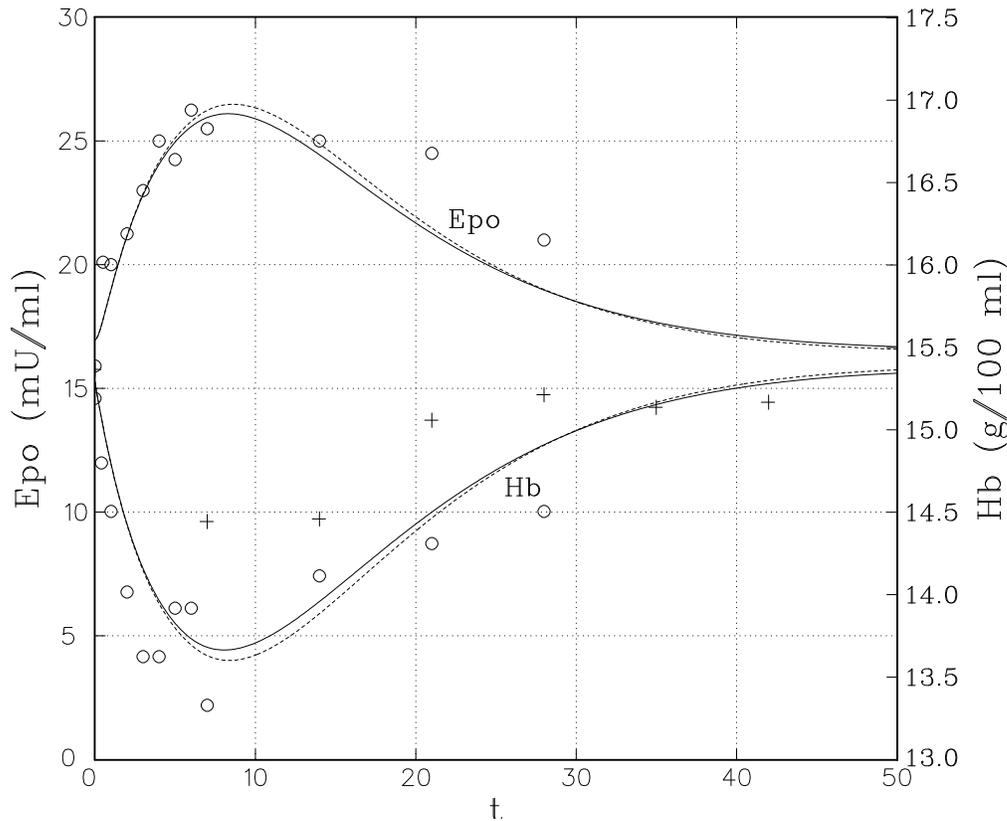


Figure 3.3: The solid curves show the age-structured model with variable velocity, while the dotted curves used  $V(E) = 1$ , which are equivalent to the graphs in Fig. 3.1 and 3.2. The data are shown for comparison.

Our next study examines the effects of including a variable velocity of aging to an age-structured model for an induced autoimmune hemolytic anemia in rabbits. Mahaffy *et al.* [25] fit their age-structured model to the experimental data of Orr *et al.* [30], where rabbits were given iso-antibodies to their erythrocytes, which in our model simply increases the value of  $\gamma$ . The study in this paper takes the model from the previous work with the same parameters that fit the experimental data, then determines what effect the inclusion of a variable velocity has on the simulation. No attempt was made to find parameters that fit the age-structured model with variable velocity to the data of Orr *et al.* [30]. Furthermore, calculations show that an equivalent model to Mahaffy *et al.* [25] including the hemoglobin function (2.6) yields negative parameters in (2.10), so the simulation presented here uses the model in Mahaffy *et al.* [25] with the mature population  $M(t)$  instead of  $Hb(t)$  in (2.9).

Fig. 3.4 shows simulations of the age-structured model with  $h = 0.02$  and velocities  $V(E) = 1$  and varying, as given by (3.2) with  $\kappa_2 = 35.5$  to match the anemic equilibrium of  $\bar{M} = 2.63$  and  $\bar{E} = 71.1$ . This graph shows that a variable velocity of maturation has a significant stabilizing influence on the model. This result is surprising, since both models have  $V(\bar{E}) = 1$  at equilibrium and all other parameters are the same. Thus, our numerical simulations show that  $V'(\bar{E})$  has a role in the stability analysis of the age-structured model. From a physiological perspective, our study suggests that by varying the rate of maturing for hematopoietic cell lines, an organism increases the stability of homeostasis for that type of cell.

The numerical simulation pointed to an error in the work of Mahaffy *et al.* [25] concerning the history used in the initial data for the delay differential equation, which is equivalent to the age-structured model with  $V(E) \equiv 1$ . The previous work used an initial history with  $E(t) = 10$  for  $-(T_1 + \bar{\nu}_F) \leq t \leq 0$ . However, the history in the initial data for the delay differential equation must reflect the information contained in the age structure of the precursor and mature populations at  $t = 0$ . Since (2.12) only uses past information on  $E(t)$ , the initial data is found by choosing the appropriate levels of Epo needed to generate the information stored in the age-structured populations. The age-structured populations at  $t = 0$  are assumed to come from normal rabbits, which have a destruction rate  $\gamma = 0.001$ , thus their mature cells have a distribution  $m(\nu) = m_0 e^{-0.001\nu}$  with  $m_0 = 0.07176$  and  $0 \leq \nu \leq \nu_F$ . An appropriate equilibrium distribution can be made for the precursor cells. However, at  $t = 0$ , the experiment assumes that  $\gamma$  jumps to 0.065 and  $\bar{M}$  shifts from 3.5 to 2.63. For  $E(t)$  to reflect the distribution for  $m(\nu)$  at  $t = 0$  with  $\gamma = 0.065$ , we take  $E(t) = 704e^{-0.064t}$ ,  $-\bar{\nu}_F \leq t \leq 0$ , which accounts for the difference in the values of  $\gamma$  before and after  $t = 0$ . A related extension accounts for the precursor population. Thus, the easier to simulate delay differential equation (2.12) may have a difficult history to analyze, while the computer simulation of the age-structured model has a more complicated algorithm with poorer convergence, but easier modeling interpretation.

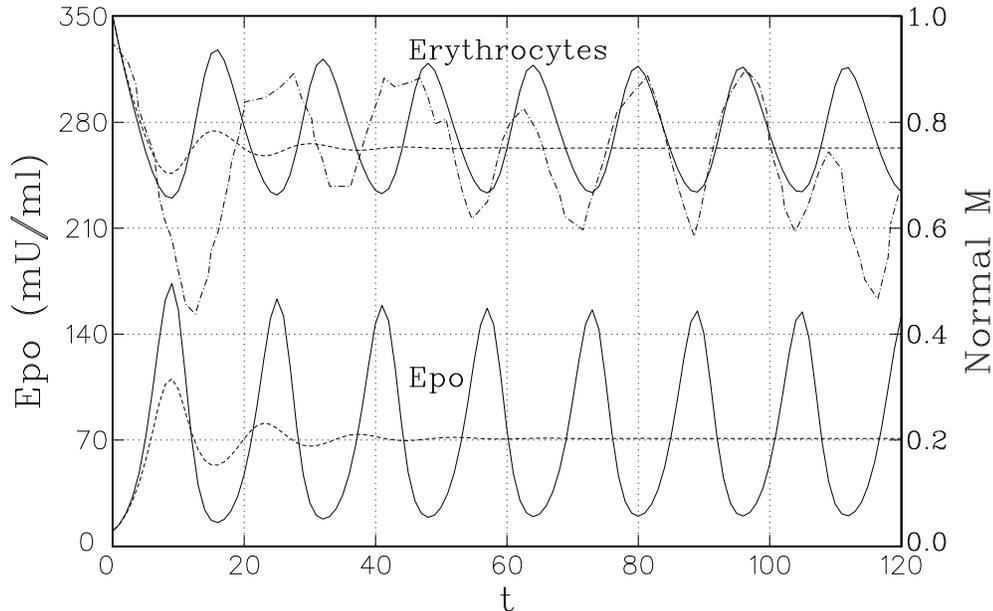


Figure 3.4: The dashed curve shows the age-structured model with variable velocity, while the solid curve used  $V(E) = 1$ . The data from Orr *et al.* is shown (dot and dash curve) and has similar oscillatory behavior to the  $V(E) = 1$  curve.

## 4 Blood Donation Experiment and Discussion

The mathematical model for a phlebotomy seems to follow the data of Maeda *et al.* [24] and Wadsworth [38] fairly well. This suggests that the model could test different blood collection schemes or enhancements through Epo injections for obtaining more blood. However, the data that was used only provided a small sample with relatively large error bars, lowering the confidence in the mathematical model. This led the authors to wonder how well the model tracked an individual.

The authors were unable to obtain data on the individuals listed in the Maeda *et al.* [24] and Wadsworth [38] data, so with the help of the San Diego Blood Bank, two of the authors donated blood, then had their hemoglobin followed for eight weeks. The data in Fig. 4.1 show the results of this informal study, overlaying the simulation of our model. These data clearly do not show the general trend of the average data from the previous section, which was used to find the best parameters for our model. There remains the general trend at the beginning of the data for the hemoglobin to drop immediately following a blood donation, but this effect is very short lived. In fact, both authors saw a return to almost normal starting hemoglobin concentrations in 4 or 5 days. Soon the data follows an almost random pattern with a mean of 14.66 and 15.10 (g/100 ml) for Mahaffy and Polk, respectively. (The standard deviation was 0.86 and 0.91 for Mahaffy and Polk, respectively.) The subjects of this study were not in a controlled experiment, so their diet and exercise regimes varied significantly (though measurements were taken at the same time each day).

The data in Fig. 4.1 show that our individual hemoglobin measurements are significantly more complicated than the data generated by the mathematical model (2.12). Since erythrocytes have the important role of carrying  $O_2$  to all tissues in the body, one expects multiple controls with different time scales affecting the concentration of hemoglobin in the blood. While brain damage begins only minutes after the cessation of a blood supply, the process of erythropoiesis takes six days. Thus, other physiological controls on the blood supply are needed to adapt to sudden changes in demand for  $O_2$  by the body tissues. As an example, one control discussed by Finch *et al.* [9] uses “shift reticulocytes” to rapidly introduce new erythrocytes to the body following a hemorrhage.

Environmental effects are clearly significant and dominate the process of erythropoiesis over shorter periods of time. For example, a phlebotomy often causes changes in the rate of hydration or urination in the subject, which directly effects blood plasma levels. In Fig. 4.1, the authors observed that the hemoglobin level dropped significantly for both participants following a day that included heavy exercise. Though initially this is counterintuitive, it becomes clear when thinking of blood as a viscous fluid. If the body needs more  $O_2$  in the tissues, then it can accomplish this by decreasing the viscosity of the blood and having the blood flow more rapidly to the tissues, which it can do readily by shifting interstitial fluid to the blood plasma. However, over a longer term the body would want to increase the concentration of erythrocytes, so that the heart would not have to pump as hard.

Several studies [29, 33, 40, 44] have been conducted comparing the blood of indigenous people living at high elevations. Amerindians (Quechua Indians) living in Peru and Himalayan natives (Sherpas) of Nepal both live at elevations exceeding 4000 m with the former being significantly more recent inhabitants to this elevation. Researchers have wondered how these people adapt to such extremes. Apparently, the Sherpas have similar hematocrit to average human populations by evolving an improved hemoglobin for carrying  $O_2$ . In contrast, the Quechua Indians have not adapted as well and have problems with polycythemia, which is a situation where the hematocrit is too high and patients have increased incidents of strokes, heart disease, and pulmonary edema. Both populations have more blood problems due to modest hypoxic hyperventilation and respiratory alkalosis. The studies of these populations show additional complications in determining the controls of erythropoiesis.

The experiments tracked in Fig. 3.1 and 4.1 show the hemoglobin lower after 56 days, suggesting less than complete recovery after eight weeks, unlike the model. However, Mahaffy is a regular blood donor at the San Diego Blood Bank, and over a 40 month period (7/95–11/98) his hemoglobin averaged 15.2 (g/100 ml) with a standard deviation of 0.85, including a high of 17.6 (g/100 ml) and low of 13.7 (g/100 ml). (Note: The high of 17.6 (g/100 ml) followed six weeks of living at 2300m elevation.) Thus, there is tremendous variability of the hemoglobin levels even at “equilibrium.”

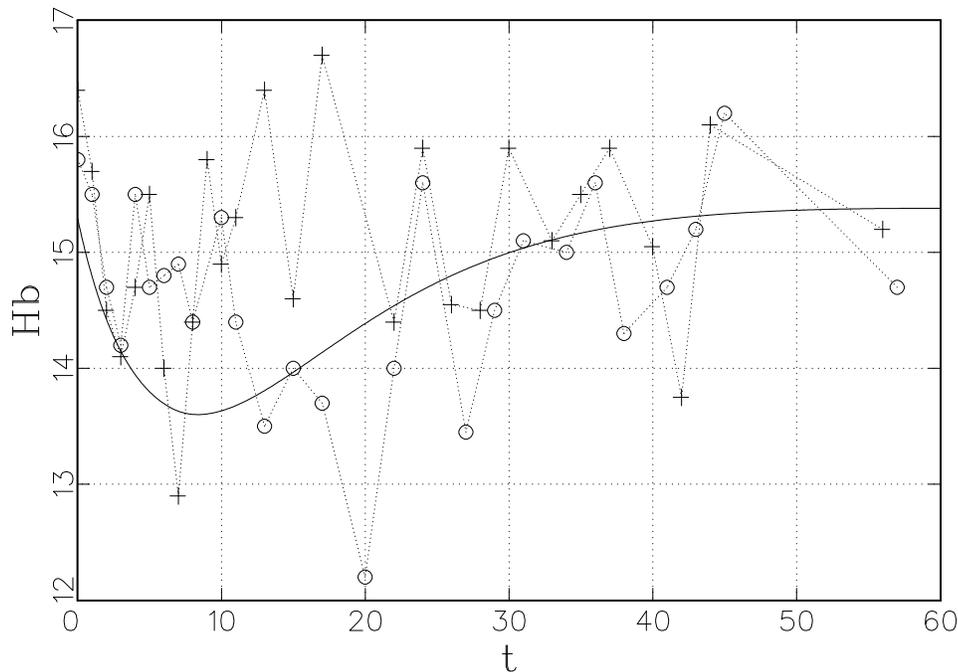


Figure 4.1: The solid curve shows the level of hemoglobin following a blood donation predicted by the model in Section 3. The data with  $\circ$  are from the author Mahaffy, while the data with  $+$  are from the author Polk after a blood donation at  $t = 0$ .

The complicated mix of physiological controls, including external input of diet and exercise, makes a complete mathematical model very difficult at this time. For example, iron is a dietary element known to significantly effect the process of erythropoiesis (and is the primary reason Blood Banks require eight weeks between donations), yet iron's role is not included in the model. By including the effects of plasma volume and concentration dependent sensing of  $O_2$ , this study has improved the mathematical model of Mahaffy *al.* [25] for phlebotomized normal human subjects to better match data. The mathematical model works well describing the cumulative data of Maeda *et al.* [24] and Wadsworth [38] and agrees with an intuitive understanding for the control of erythropoiesis following a phlebotomy. Our numerical work demonstrates that the variable velocity of aging for the precursor cells has a minimal effect on the qualitative behavior of the model for normal human subjects, thus the simplified delay differential equation model is adequate for a basic understanding of erythropoietic controls following a phlebotomy. Still, the environmental factors dominate the changes in concentrations of hemoglobin and Epo, making our models inappropriate for determining better blood donation schemes.

Our comparative studies of the induced autoimmune hemolytic anemia for rabbits were particularly interesting. Mahaffy *al.* [25] simulated the experiments of Orr *et al.* [30] on rabbits with hemolytic anemia using a system of delay differential equations similar to (2.12). When we used the complete age-structured model and included the variable velocity of aging for the precursor cells, there was a significant increase in the stability of the mathematical model, as shown in Fig. 3.4. Further mathematical studies are needed to explain how this addition to the model effects stability. Biologically, this increased stability is clearly a favorable adaptation from an evolutionary point of view for maintaining homeostasis of erythrocytes.

Our numerical studies show that a simplified delay differential equation is much easier to examine, particularly when fitting parameters to the model. However, the age-structured model is easier to interpret biologically. Both models for erythropoiesis provide clues for disease states centered around stem cells, and though they are inappropriate for improving blood donation schemes, they assist in the understanding of

one major part of the regulatory process of carrying  $O_2$  to the tissues.

---

Special thanks to the San Diego Blood Bank for their assistance with the hematocrit study of the authors. Their nursing staff was very cooperative, amiable, and informative for the duration of our experiment. Also, the authors recognize the assistance of Danielle Brown and Edward Trovato who were supported under the REU program of NSF by grant DMS-9208290.

## References

- [1] America's Blood Centers, 1998. Facts on Blood, [www.americasblood.org/facts/frame.htm](http://www.americasblood.org/facts/frame.htm), Puget Sound Blood Center.
- [2] J. Bélair, M. Mackey, and J. M. Mahaffy. Age-structured and two-delay models for erythropoiesis. *Math. Biosci.*, 128:317–346, 1995.
- [3] E. Beutler, M. A. Lichtman, B. S. Coller, and T. J. Kipps. *William's Hematology*. McGraw-Hill, New York, 5<sup>th</sup> edition, 1995.
- [4] S. Busenberg, K. Cooke, and M. Iannelli. Endemic thresholds and stability in a class of age-structured epidemics. *SIAM J. Appl. Math.*, 48:1379–1395, 1988.
- [5] S. Busenberg and M. Iannelli. Separable models in age-dependent population dynamics. *J. Math. Biol.*, 22:145–173, 1985.
- [6] O. Diekmann and J. A. J. Metz. On the reciprocal relationship between life histories and population dynamics. In S.A. Levin, editor, *Frontiers in Theoretical Biology. volume 100 Lecture Notes in Biomathematics*, pages 19–22. Springer-Verlag, Berlin and New York, 1994.
- [7] C. D. R. Dunn. Cyclic hematopoiesis: The biomathematics. *Experimental Hematology*, 11:779–791, 1983.
- [8] A. J. Erslev. Production of erythrocytes. In M.M. Williams, editor, *Hematology*, pages 389–397. McGraw-Hill, New York, 4<sup>th</sup> edition, 1990.
- [9] C. A. Finch, L. A. Harker, and J. D. Cook. Kinetics of the formed elements of human blood. *Blood*, 50:699–707, 1977.
- [10] J. A. Gatica and P. Waltman. A threshold model of antigen antibody dynamics with fading memory. In V. Lakshmikantham, editor, *Nonlinear Phenomena in Mathematical Sciences*. Academic Press, New York, 1982.
- [11] J. A. Gatica and P. Waltman. A system of functional differential equations modeling threshold phenomena. *Appl. Anal.*, 28:39–50, 1988.
- [12] R. R. Gordon and S. Varadi. Congenital hypoplastic anemia (pure red cell anemia) with periodic erythroblastopenia. *Lancet*, i:296–299, 1962.
- [13] A. Grabosch and H. J. A. M. Heijmans. Cauchy problems with state-dependent time evolution. *Japan J. Appl. Math.*, 7:433–457, 1990.
- [14] A. Grabosch and H. J. A. M. Heijmans. Production, development and maturation of red blood cells. A mathematical model. In D.E. Axelrod O. Arino and M. Kimmel, editors, *Mathematical Population Dynamics*, pages 189–210. Marcel Dekker, New York, 1991.

- [15] R. S. Hill. Characteristics of marrow production and reticulocyte maturation in normal man in response to anemia. *J. Clin. Invest.*, 48:443–453, 1969.
- [16] N. D. Kazarinoff and P. van den Driessche. Control of oscillations in hematopoiesis. *Science*, 203:1348–1350, 1979.
- [17] E. A. King-Smith and A. Morley. Computer simulation of granulopoiesis. *Blood*, 36:254–262, 1970.
- [18] J. Kirk, J. S. Orr, and C. S. Hope. A mathematical analysis of red blood cell and bone marrow stem cell control mechanisms. *British Journal of Haematology*, 15:35–46, 1968.
- [19] S. Labardini, Th Papayannopoulou, J. D. Cook, J. W. Adamson, R. D. Woodson, J. W. Eschbach, and R. S. Hill. Marrow radioiron kinetics. *Haematologia*, 7:301–312, 1973.
- [20] M. C. Mackey. A unified hypothesis for the origin of aplastic anemia and periodic haematopoiesis. *Blood*, 51:941–956, 1978.
- [21] M. C. Mackey. Dynamic haematological disorders of stem cell origin. In J. G. Vassileva-Popova and E. V. Jensen, editors, *Biophysical and Biochemical Information Transfer in Recognition*, pages 373–409. Plenum Publishing Corp., New York, 1979.
- [22] M. C. Mackey. Periodic auto-immune hemolytic anemia: An induced dynamical disease. *Bull. Math. Biol.*, 41:829–834, 1979.
- [23] M. C. Mackey and J. G. Milton. Feedback, delays and the origin of blood cell dynamics. *Comments Theor. Biol.*, 1:299–327, 1990.
- [24] H. Maeda, Y. Hitomi, R. Hirata, H. Tohyama, J. Suwata, S. Kamata, Y. Fujino, and N. Murata. The effect of phlebotomy on serum erythropoietin levels in normal healthy subjects. *Int. J. Hemat.*, 55:111–115, 1992.
- [25] J. M. Mahaffy, J. Bélair, and M. Mackey. Hematopoietic model with moving boundary condition and state dependent delay: Applications in erythropoiesis. *J. theor. Biol.*, 190:135–146, 1998.
- [26] J. A. J. Metz and O. Diekmann. *The Dynamics of Physiologically Structured Populations*, volume 68 Lecture Notes in Biomathematics. Springer-Verlag, Berlin, 1986.
- [27] F. D. Moore. The effects of hemorrhage on body composition. *New Eng. J. Med.*, 273:567–577, 1965.
- [28] A. Morley. Cyclic hemopoiesis and feedback control. *Blood Cells*, 5:283–296, 1979.
- [29] G. Morpurgo, P. Arese, A. Bosia, G. P. Pescarmona, M. Luzzana, G. Modiano, and S. Krishnarajit. Sherpas living permanently at high altitude: A new pattern of adaptation. *Proc. Natl. Acad. Sci. USA*, 73(3):747–751, 1976.
- [30] J. S. Orr, J. Kirk, K. G. Gray, and J. R. Anderson. A study of the interdependence of red cell and bone marrow stem cell populations. *Brit. J. Haemat.*, 15:23–34, 1968.
- [31] Th Papayannopoulou and C. A. Finch. Radio-iron measurements of red cell maturation. *Blood Cells*, 1:535–546, 1975.
- [32] P. Ranlov and A. Videbaek. Cyclic haemolytic anaemia synchronous with pel-ebstein fever in a case of hodgkin’s disease. *Acta Medica Scandinavica*, 174:583–588, 1963.
- [33] R. B. Santolaya, S. Lahiri, R. T. Alfaro, and R. B. Schoene. Respiratory adaptation in the highest inhabitants and highest sherpa mountaineers. *Respir. Physiol.*, 77:253–62, 1989.

- [34] G. K. von Schulthess and N. A. Mazer. Cyclic neutropenia (CN): A clue to the control of granulopoiesis. *Blood*, 59:27–37, 1982.
- [35] H. L. Smith. Reduction of structured population models to threshold-type delay equations and functional differential equations: A case study. *Math. Biosci.*, 113:1–23, 1993.
- [36] D. Sulsky. Numerical solution of structured population models: I Age structure. *J. Math. Biol.*, 31:817–839, 1993.
- [37] D. Sulsky. Numerical solution of structured population models: II Mass structure. *J. Math. Biol.*, 32:491–514, 1994.
- [38] G. R. Wadsworth. Recovery from acute haemorrhage in normal men and women. *J. Physiol.*, 129:583–593, 1955.
- [39] M. Wazewska-Czyzewska. *Erythrokinetics*. National Technical Information Service, Springfield VA, 1984.
- [40] J. B. West. Respiratory and circulatory control at high altitudes. *J. Exp. Biol.*, 100:147–157, 1982.
- [41] T. E. Wheldon. Mathematical models of oscillatory blood cell production. *Math. Biosci.*, 24:289–305, 1975.
- [42] T. E. Wheldon, J. Kirk, and H. M. Finlay. Cyclical granulopoiesis in chronic granulocytic leukemia: A simulation study. *Blood*, 43:379–387, 1974.
- [43] H. E. Wichmann and M. Loeffler. *Mathematical Modeling of Cell Proliferation: Stem Cell Regulation in Hemopoiesis*. CRC Press, Boca Raton, 1988.
- [44] R. M. Winslow, K. W. Chapman, C. C. Gibson, M. Samaja, C. C. Monge, E. Goldwasser, M. Sherpa, F. D. Blume, and R. Santolaya. Different hematologic responses to hypoxia in sherpas and quechua indians. *J. Appl. Physiol.*, 66:1561–1569, 1989.